 doi:10.20944/preprints202010.0239.v1

Article

Influence of cholesterol on the orientation of the farnesylated GTP-bound KRas-4B binding with anionic model membranes

Huixia Lu [1], Jordi Martí [1]*

[1] Affiliation: Department of Physics, Technical University of Catalonia-Barcelona Tech, Barcelona, Spain.
* Correspondence: jordi.marti@upc.edu

Abstract: The Ras family of proteins is tethered to the inner leaflet of the cell membranes which play an essential role in signal transduction pathways that promote cellular proliferation, survival, growth, and differentiation. KRas-4B, the most mutated Ras isoform in different cancers, has been under extensive study for more than two decades. Here we have focused our interest on the influence of cholesterol on the orientations that KRas-4B adopts with respect to the plane of the anionic model membranes. How cholesterol in the bilayer might modulate preferences for specific orientation states is far from clear. Herein, after analyzing data from in total 4000 ns-long MD simulations for four KRas-4B systems, properties such as the area per lipid and thickness of the membrane as well as selected radial distribution functions, penetration of different moieties of KRas-4B, and internal conformational fluctuations of flexible moieties in KRas-4B have been calculated. It has been shown that high cholesterol content in the PM favors OS_1, exposing the effector-binding loop for signal transduction in the cell from the atomic level. We confirm that high cholesterol in the PM helps KRas-4B mutant stay in its constitutively active state, which suggests that high cholesterol intake can increase mortality and may promote cancer progression for cancer patients. We propose that during the treatment of KRas-4B-related cancers, reducing the cholesterol level in the PM and sustaining cancer progression by controlling the plasma cholesterol intake might be taken into account in anti-cancer therapies.

Keywords: KRas-4B; mutation; post-translational modification; HVR; anionic plasma membrane; signaling; cholesterol.

1. Introduction

Plasma membrane (PM) systems have been extensively studied over several decades [1–5] on their association with proteins. Recent studies have shown that the role of proteins and their interactions with components of PM is extremely important to understand the mechanisms of protein anchoring into the membrane that can lead to oncogenesis [6]. GTPases are a large family of hydrolase enzymes that bind to the nucleotide guanosine triphosphate (GTP) and hydrolyze it to guanosine diphosphate (GDP). GDP/GTP cycling is controlled by two main classes of regulatory proteins. Guanine-nucleotide-exchange factors (GEFs) promote the formation of the active, GTP-bound form, while GTPase-activating proteins (GAPs) inactivate Ras by enhancing the intrinsic GTPase activity to promote the formation of the inactive GDP-bound form [7–9]. Ras proteins are small molecular weight GTPases and function as GDP/GTP-regulated molecular switches controlling pathways involved in critical cellular functions like cell proliferation, signaling, cell growth, and anti-apoptosis pathways [10]. The three Ras genes give rise to three base protein sequences: KRas, HRas, and NRas. Over 30% of cancers are driven by mutant Ras proteins, thereinto, one method called Catalog of Somatic Mutations in Cancer (COSMIC) [11] confirms that HRas (3%) is the least frequently mutated Ras isoforms in human cancers, where KRas (86%) is the predominantly mutated isoforms followed by NRas (11%) [12].

 doi:10.20944/preprints202010.0239.v1

KRas can be found as two splice variants designated KRas-4A and KRas-4B. They both have polybasic sequences that facilitate membrane-association in acidic membrane regions [13], however, for KRas-4A it is covalently modified by a single palmitic acid. KRas-4B is distinguished from KRas-4A isoform in the residue 181 that serves as a phosphorylation site within its flexible hypervariable region (HVR, residues 167-185) that contains the farnesyl group (FAR) serving as the lipid anchor. The HVR of KRas-4B contains multiple amino-acid lysines that act as an electrostatic farnesylated switch which guarantees KRas-4B's association with the negatively charged phospholipids in the inner PM leaflet. It has been reported that the KRas-4B activation level in diseased cells is linked to phosphatidylserine contents [14]. Anionic lipids could influence the membrane potential which in turn regulates the orientation, location, and signaling ability of KRas-4B [15,16].

The catalytic domain (CD, residues 1-166), which contains the catalytic lobe (lobe 1, residues 1-86) and the allosteric lobe (lobe 2, residues 87-166), highly homologous, conserved, and the structure is shared and identical for KRas-4A and KRas-4B. According to P. Prakash *et al* [17–19], three distinct orientation states of the oncogenic G12V-KRas-4B mutant on the membrane have been reported, namely, OS_1, OS_2, and OS_0. OS_1, with an accessible effector-binding loop, and OS_2, with the effector-binding loop occluded by the membrane, have been reported. They differ in the accessibility of functionally critical switch loops to the downstream effectors, suggesting that membrane reorientation of KRas-4B on the inner cell leaflet may modulate its signaling [18]. The idea of the more flexible in the structure of proteins, the larger the number of their populated states have been pointed out [20]. We and other researchers have recently shown that despite the HVR and FAR anchor, the CD of KRas-4B could interact with anionic model membranes by forming steady salt-bridges and hydrogen-bonds to help organize its orientations in cells [15,21,22].

All Ras proteins' signaling strongly depends on their correct localization in the cell membrane and it is essential for activating downstream signaling pathways. KRas-4B function, membrane-association and interaction with other proteins are regulated by post-translational modifications (PTMs) [23–25], including ubiquitination, acetylation, prenylation, phosphorylation, and carboxymethylation, see Fig. 1. Firstly the prenylation reaction, catalyzed by cytosolic farnesyltrasferase (FTase) or geranylgeranyltransferase (GGTase), proceeds through the addition of an isoprenyl group to the Cys-185 side chain. Then farnesylated KRas-4B is ready for further processing: hydrolysis, catalyzed by the endopeptidase enzyme called Ras-converting enzyme 1 (RCE1), during the process the VIM motif (HVR tail composed of three amino acids: valine-isoleucine-methionine) of the C-terminal Cys-185 is lost in step 2.

Preprints (www.preprints.org) | NOT PEER-REVIEWED | Posted: 12 October 2020 doi:10.20944/preprints202010.0239.v1

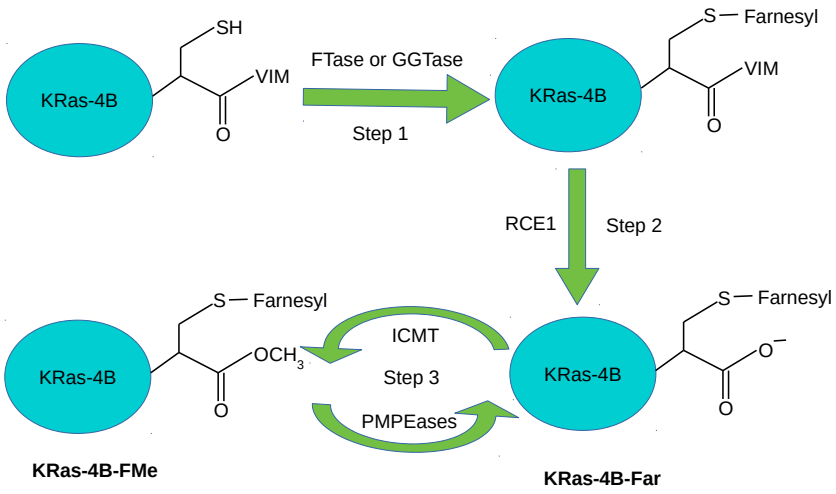

Figure 1. PTMs steps of KRas-4B: prenylation, hydrolysis, carboxymethylation and decarboxymethylation.

In step 3, KRas-4B is transferred to the endoplasmic reticulum for carboxymethylation at the carboxyl terminus of Cys-185 catalyzed by isoprenylcysteine carboxyl methyltransferase (ICMT), forming a reversible ester bond. The reversible ester bond can go through decarboxymethylation, catalyzed by Prenylated/polyisoprenylated methylated protein methyl esterases (PMPEases) giving rise to a farnesylated and demethylated KRas-4B (KRas-4B-Far). Carboxymethylation is one of the best known reversible PTMs in HVR [26]. This reversible reaction can modulate the equilibrium of methylated/demethylated KRas-4B population (KRas-4B-FMe/KRas-4B-Far) in tumors and consequently can impact downstream signaling, protein-protein interactions, or protein-lipid interactions [27]. Another well-known reversible PTM in the HVR is phosphorylation [25,28,29]. There are two sites (Ser-171 and Ser-181) within HVR that could be phosphorylated. Phosphorylation involves the addition of phosphate (PO_4^{3-}) group to the side. Phosphorylation at Ser-181 operates a farnesyl-electrostatic switch that reduces but does not completely inhibit membrane-association and clustering of KRas-4B, leading to redistribution to the cytoplasm and endomembranes [24,30,31]. Functionally, phosphorylation of KRas-4B can have either a negative [32,33] or positive [31,34] regulatory effect on the tumor cell growth, depending on the conditions [27]. For instance, from an MD simulation of the HVR peptide with the FAR at Cys-185 of KRas-4B in two types of model membranes, it has been observed that phosphorylation at Ser-181 prohibits spontaneous FAR membrane insertion [35]. According to Agell *et al*. KRas-4B binding with calmodulin leads to different behaviors: short or prolonged signaling whether KRas-4B is at its phosphorylated state on residue Ser-181 [31,36]. chain of the amino acid serine, then the phosphorylated serine (PHOS) is obtained. Moreover, according to Barcelo *et al*. [34], phosphorylation at Ser-181 of oncogenic KRas is required for tumor growth. In summary, phosphorylation of the HVR of KRas-4B can affect its function, membrane-association, and reacting with downstream effectors [27].

Phosphodiest-eraseδ (PDEδ) has been revealed to promote effective KRas-4B signaling by sequestering KRas-4B-FMe from the cytosol by binding the prenylated HVR and help to enhance its diffusion to the PM throughout the cell, where it is released to activate various signaling pathways required for the initiation and maintenance of cancer [37–40], hoping to identify a panel of novel PDEδ inhibitors. As described in our earlier work [21], despite KRas-4B-Far's poor affinity for PDEδ [37], it can still be transferred to the PM through trapping and vesicular transport without the help of PDEδ [41]. Moreover, According to Ntai *et al*. 91% of the mutant KRas-4B and 51% of wild-type KRas-4B

Preprints (www.preprints.org) | NOT PEER-REVIEWED | Posted: 12 October 2020 doi:10.20944/preprints202010.0239.v1

proteins in certain colorectal tumor samples have been found to exist in its KRas-4B-Far form. While there is a relatively high abundance of KRas-4B-Far (wild-type and mutant) lacking the methyl group of Cys-185 in tumors, the effects of demethylated KRas-4B-Far on downstream signaling have yet to be determined [42]. While extensive research has been focused on methylated KRas-4B-FMe, we believe that demethylated KRas-4B-Far could play a big role in the signaling pathway that happens on the inner leaflet of the membrane bilayers.

Cholesterol plays an important role in maintaining the structure of different membranes and regulating their functions [43,44], and cancer development as well [45]. The fluidity of the membrane is mainly regulated by the amount of cholesterol, in such a way that membranes with high cholesterol contents are stiffer than those with low amounts but keeping the appropriate fluidity for allowing normal membrane functions. Extensive research has been done on the influence of cholesterol on the mechanism of membrane structures [46], the 18-kDa translocator protein (TSPO) binding in the brain [47], etc. There is evidence that shows that high cholesterol increases pancreatic cancer risk [48], but it doesn't influence the mortality among patients with pancreatic cancer [49]. In this work, We have investigated whether cholesterol in membranes affects the signaling of Ras proteins by interfering with their orientations when the oncogenic and wild-type KRas binding with the membrane. Gaining a precise understanding of the influence of cholesterol on the reorientation of mutant and wild-type KRas-4B-Far binding at the anionic model membranes is the goal of the current work.

2. Results and discussion

2.1. Area per lipid

Area per lipid is often used as the key parameter when assessing the validity of MD simulations of cell membranes. It has been proposed that a good test for such validation is the comparison of the area per lipid and thickness of the membrane with experimental data obtained from scattering density profiles [50]. The area per lipid and thickness along the simulation time of the last 500 ns have been computed (see Fig. A1 of supporting information (SI)) and the average values are reported in Table 1.

Table 1. The average area per lipid (A) and thickness (Δz) of the anionic membrane for four KRas-4B-Far systems studied in this work. The thickness of the membrane Δz by computing the mean distance between phosphorus atoms of the DOPC head groups from both leaflets. Estimated errors in parenthesis.

System	A (nm^2)	Δz (nm)
wt. chol.-0%	0.679 (0.008)	3.84 (0.04)
wt. chol.-30% [21]	0.523 (0.007)	4.35 (0.05)
onc. chol.-0%	0.679 (0.008)	3.89 (0.04)
onc. chol.-30% [21]	0.525 (0.006)	4.23 (0.04)

The experimental value of 0.71 nm^2 for area per lipid of DOPC/DOPS (4:1) at 297 K was reported in Ref. [51] and the experimental value of thickness to be of 3.94 nm at 303 K was reported by Novakova *et al*. [52]. As temperature increases, atoms in the lipid structure oscillate more perpendicularly to their bonds. So increasing the temperature of the system leads to an increased area per lipid of certain phosphatidylcholine lipids as it was observed for temperatures below 420 K [53]. It was previously reported that KRas-4B can interact with head groups of DOPC and DOPS lipid molecules through long-lived salt bridges and hydrogen-bonds [21]. Accordingly, when the system temperature rises, for the same model membrane, its thickness decreases. Our results of the area per lipid (0.03 nm^2) and thickness ($\sim$ 0.1 nm) are smaller than the experiment values for pure lipid systems. The main reason is the contribution of the joint effect of raising the system temperature and the appearance of KRas-4B-Far, showing a slight condensing effect on the membrane. According to earlier research [54], in the case

Preprints (www.preprints.org) | NOT PEER-REVIEWED | Posted: 12 October 2020 doi:10.20944/preprints202010.0239.v1

of relative high cholesterol concentration, 10 $\sim$ 20% smaller area per lipid will be considered to be reasonable and close to equilibrium ones. From another work [55], compared to pure DMPC bilayer, the area per lipid of DMPC with cholesterol (30%) has been decreased by 32% from 0.62 to 0.42 nm^2. In the regime with chol. $\leq$ 30%, the area per lipid has been reported to decrease sharply as cholesterol is added into the system [56]. In Table 1, the area per lipid for high cholesterol cases (chol.-30%) has been decreased by 23% when compared with the cholesterol-free cases (chol.-0%). The results make much sense when compared with the experimental values confirming cholesterol's condensation effect on DOPC/DOPS membrane bilayers. The results of the area per lipid and thickness of membrane bilayers we have investigated are in good agreement with experimental values. Hence, the validity of MD simulations reported here, regarding the structural characteristics of the membrane, has been established.

2.2. Preferential localization of KRas-4B-Far on membranes

Ras proteins are activated following an incoming signal from their upstream regulators and interact with their downstream effectors only when they are anchored into the membrane and being at the GTP-bound state. Tracking the movement of the FAR of KRas-4B-Far and GTP along the membrane normal could give us the direct information of how does the KRas-4B proteins and GTP molecule regulate. We report in Fig. 2, the Z-axis positions of the centers of FAR and GTP from the center of lipids (i.e. Z = 0) using the second half of 1000 ns simulation for all cases.

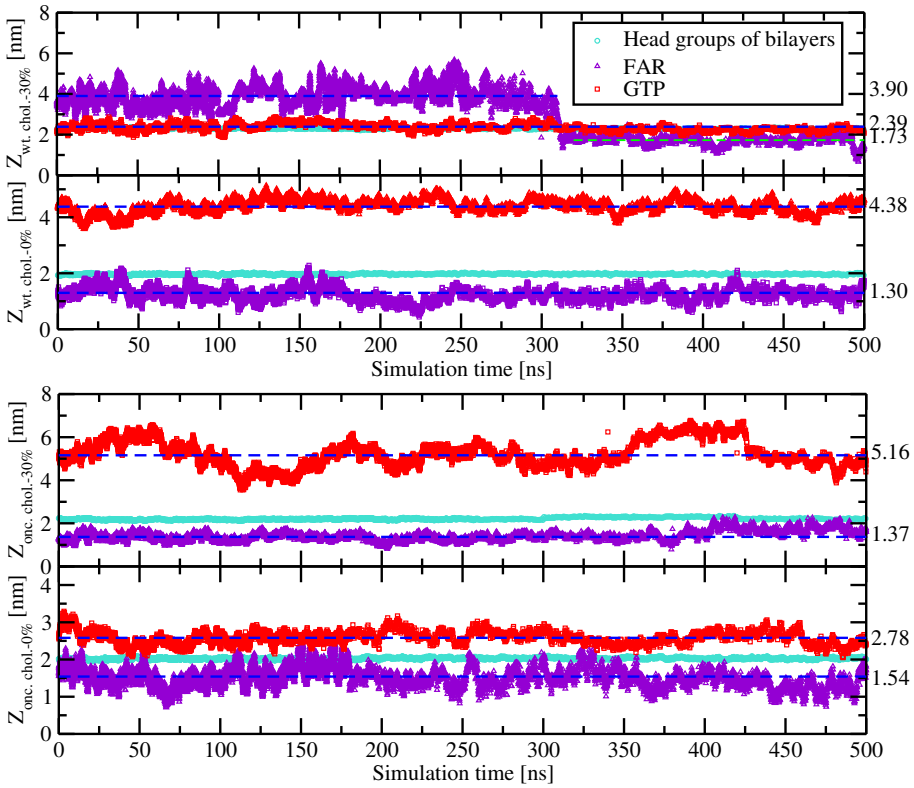

Figure 2. The localizations of the FAR and GTP of four KRas-4B systems studied in this work with respect to the center of the membrane along with the membrane normal as a function of simulation time. Geometric centers of the FAR, GTP, and phosphorus atoms of DOPC lipids from both leaflets are indicated as triangle up in violet and circle in turquoise, respectively. Data for chol.-30% shown here are adopted from our previous work [21] for the convenience of the audience. The average value of the FAR and GTP are indicated in the blue dashed line.

As is described in Ref. [21], the FAR of the wild-type KRas-4B-Far is revealed to be able to anchor into and depart from the membrane without difficulty in the chol.-30% case when GTP favors binding

 doi:10.20944/preprints202010.0239.v1

with the interface of the membrane through salt-bridges and hydrogen-bonds, located at around 2.39 nm from the membrane center. The FAR can have two preferred localisations: 1) 3.90 nm when FAR wanders in the water region, and 2) 1.73 nm when FAR anchors inside of the PM. However, in the chol.-free case, the FAR of the wild-type KRas-4B-Far is found to be anchoring constantly into the anionic membrane for the entire duration of the simulations. FAR keeps locating around 1.30 nm, while GTP keeps binding to the CD, staying around 4.38 nm.

For the mutant KRas-4B-Far, when diffusing in the DOPC/DOPS (4:1) bilayer, GTP tends to wander around 2.78 nm away from the membrane center along with the membrane normal direction. When 30% of cholesterol was considered, GTP favors binding with the CD instead of wandering near the interface region of the membrane. For both oncogenic cases, FAR is revealed to be anchoring constantly into the anionic membrane as a function of the simulation time, as might be expected.

By comparing the four systems we studied, we propose that adding cholesterol into the system has less influence on the behavior of FAR of the oncogenic KRas-4B-Far anchoring to the anionic membrane. And for a different type of KRas-4B-Far, GTP's localization can't be predicted according to different types of mutations in the KRas-4B's structure and the constitution of the cell membrane we are studying. Remarkably, the existence of cholesterol helps FAR of the mutant KRas-4B-Far anchor 0.17 nm deeper into the anionic membrane than the chol.-0% case.

2.3. Conformation of the 5-aa-sequence in the HVR

As suggested by Dharmaiah *et al* [37], a 5-amino-acid-long sequence motif in its HVR (K-S-K-T-K, residues 180-184), which is shared by KRas-4B-Far and KRas-4B-FMe, may enable PDEδ to bind prenylated KRas-4B.

The root mean square deviation of certain atoms in a molecule with respect to a reference structure, defined as Eq. 1, is the most commonly used quantitative measure of the similarity between two superimposed atomic coordinates [57].

$$RMSD = \sqrt{\frac{1}{n}\sum_{i=1}^{n} d_i^2} \tag{1}$$

where d_i is the distance between the two atoms in the i-th pair and the averaging is performed over the n pairs of atoms.

A closer investigation of RMSD of this 5-aa-sequence of the HVR of two KRas-4B-Far (wt. and onc.) binding to two different anionic model membranes has been done.

Preprints (www.preprints.org) | NOT PEER-REVIEWED | Posted: 12 October 2020 doi:10.20944/preprints202010.0239.v1

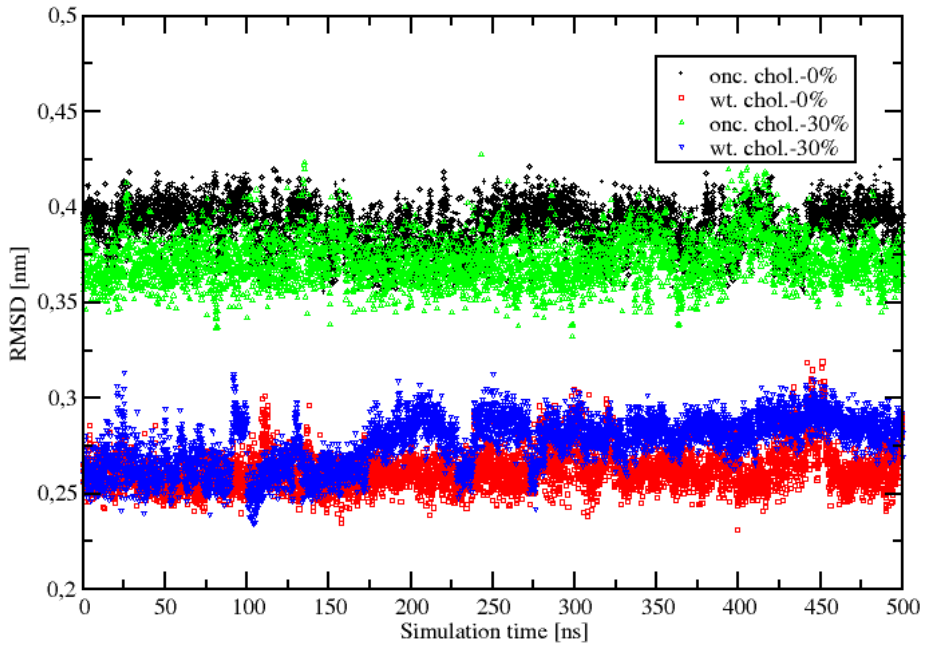

Figure 3. Backbone root mean square deviation (RMSD) of the 5-aa-sequence of the HVR during the last 500 ns of the 1 μs time span for four systems.

Fig. 3 presents the results of adding cholesterol into the system to their respective reference structures. Obviously, cholesterol doesn't have as much impact as two mutations in the sequence of KRas-4B on the same type of KRas-4B-Far, highlighting the significant influence of the mutations on the conformational change of the 5-aa-sequence in the HVR. It also demonstrates that for the wild-type KRas-4B-Far protein, the RMSD of the 5-aa-sequence ranges from 0.24 to 0.3 nm, and for the oncogenic one, the value ranges from 0.35 to 0.42, due to inherent structural flexibility.

2.4. KRas-4B-Far's orientation distributions on different anionic membranes

Several previous studies have shown that the orientations of Ras proteins on membranes significantly impact their function in cell [17,18,58–60]. Cell membranes are platforms for cellular signal transduction. Their structure and function depend on the composition of cholesterol and related phospholipids [61]. Furthermore, both clinical and experimental studies have found that hypercholesterolemia and a high-fat high-cholesterol diet can affect cancer development [45,62]. Increased cholesterol levels in the human body are associated with a higher cancer incidence, and reducing its level through drugs (for instance: statins) could reduce the risk and mortality of some cancers, such as prostate, colorectal, and breast cancer [63–65]. Increased serum cholesterol levels could be used as an indicator for developing cancers, such as colon, prostatic, testicular, and rectal cancer [66,67].

To explore the influence of cholesterol on the orientation of KRas, we employed the definition of the orientation of KRas-4B-FMe described by Prakash *et al* [17] to compare with the results from this work and propose a new method to define the orientation of KRas binding to the PM. In general, two order parameters have been adopted: 1) the distance (z) between C_α atoms of the residue 132 on the lobe 2 and the residue 183 on the HVR, and 2) the angle Θ between the membrane normal direction and a vector running the C_α atoms of the residue 5 and the residue 9 which belong to the first strand

Preprints (www.preprints.org) | NOT PEER-REVIEWED | Posted: 12 October 2020 doi:10.20944/preprints202010.0239.v1

β1 in the structure of KRas-4B. Two distinct orientations of KRas were proposed in their work: OS_1, in which the loop is solvent-accessible, and OS_2, in which the effector-binding loop is occluded by the membrane. The remaining conformations are categorized into the intermediate state OS_0.

Moreover, we define a new parameter, the angle Φ that runs the membrane normal and a vector running the C_α atoms of residues 163 and 156 on the last helix α5 of lobe 2. Due to its highly conserved structure for the CD, providing the information of the angle Θ along with the Φ could provide a new way for researchers to define the movement and orientation for KRas when binding to the membranes. We have calculated the angle and distance as described above. And the parameter we newly introduce here will be discussed further later.

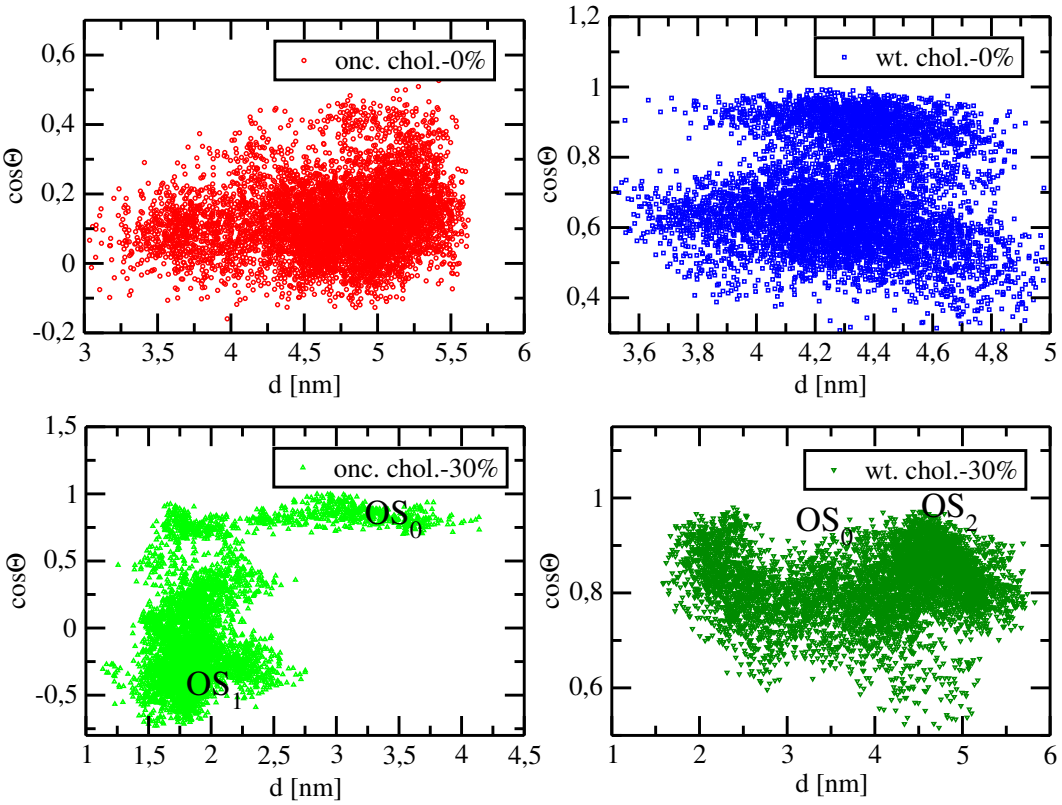

Figure 4. Density distribution of conformations defined by the order parameter z and cosΘ.

Time evolution of z for each system is reported in Fig. A2, which shows major conformational fluctuations for four systems. From the last 500 ns simulation time analyzed in this work, wild-type and mutant KRas-4B-Far proteins could reach all three conformational regions when binding to the anionic cholesterol-rich membrane, indicating more flexibility in the CD structure when the PM contains more cholesterol lipids. For the cholesterol-free membrane systems, the protein majorly fluctuates between two distinct states in ranges of $2.4 \leq z \leq 4.3$ and $z > 4.3$ nm, rarely visiting lower z values.

Through the two-dimensional histogram, (z , CosΘ), three orientation states OS_1 , OS_2, and OS_0 were found to be centered around (1.86, -0.5), (4.97, 1), and (3.33, 0.9), respectively. In Fig. 4, we can observe that only when oncogenic KRas-4B-Far is bound to the cholesterol-rich membrane, can OS_1 be shown for KRas in a time span of 500 ns. In OS_1, KRas-4B can interact with other proteins in cells, confirming that cholesterol has an important impact on the signaling activity for KRas-4B, especially for mutant ones, by increasing the flexibility and fluctuation in its CD with the exposed effector-binding loop.

As expected, the wild-type KRas-4B-Far favors staying in its inactive state (OS_2) regardless of the concentration of cholesterol in the PM. However, using these two coordinates (z, cosΘ) it becomes difficult for us to categorize their states because of the large flexibility in structure for complex proteins for the cholesterol-free systems. For the two cholesterol-free systems, are the orientation states of

Preprints (www.preprints.org) | NOT PEER-REVIEWED | Posted: 12 October 2020 doi:10.20944/preprints202010.0239.v1

wild-type and oncogenic KRas-4B-Far always in its intermediate state OS_0 according to Prakash *et al*'s work [17]? This is a question that we want to answer.

2.5. Reorientation of mutant KRas-4B-Far on the anionic membranes

By adopting the two angles (Θ and Φ) defined above we analyzed the corresponding density profiles. We present the reorientation of the mutant KRas-4B-Far when bound to the anionic membrane with 30% of the cholesterol in Fig. 5. Results for the remaining three systems studied here are reported in Figs. A3, A4, and A5 of the SI.

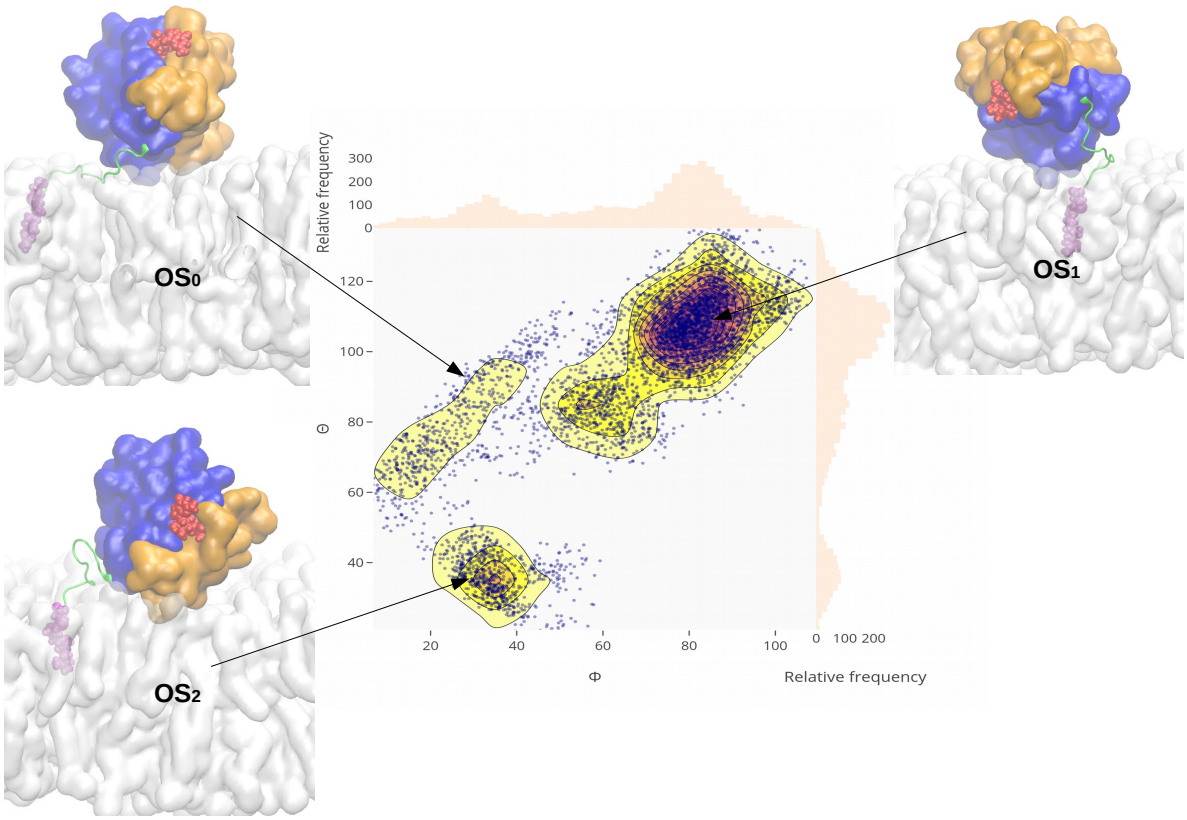

Figure 5. Reorientation of the oncogenic KRas-4B on the cholesterol-30% membrane. Density distribution of conformations projected on to a plane defined by the reaction coordinates Φ and Θ in degrees (°). The relative frequency of each coordinate is shown on the right and upsides. The membrane bilayer is shown as a white surface. Lobe 1 is highlighted in orange, lobe 2 in blue, HVR backbone in green, GTP in red, and FAR in violet. Water and ions are not shown here for the sake of clarity.

From Fig. 5, the reorientation of mutant KRas-4B-Far on the cholesterol-30% bilayer has been observed during the 500 ns simulations time, giving a hint on the low free energy barriers between two orientation states (OS_1-OS_0, and OS_0-OS_2). Mutant KRas-4B spends most of the time in the active OS_1 state, centered at (80°, 105°) on cholesterol-30% membrane, and fluctuates around (99°, 83°) when binding to the cholesterol-free bilayer, also in its OS_1 state. Wild-type KRas-4B protein, regardless of the cholesterol's content, prefers staying it its inactivate state, centered at (59°, 52.5°) and (53°, 37°) for cholesterol-0% and cholesterol-30%, respectively. This suggests that the orientation with the effector-binding loop occluded by the membrane (OS_2) is disfavored in the wild-type KRas-4B-Far protein.

Here we could conclude that high cholesterol in the PM helps KRas-4B mutant stay in its constitutively active state, which suggests that high cholesterol intake can increase the mortality

 doi:10.20944/preprints202010.0239.v1

and may promote cancer progression for cancer patients. Our findings agree with the experimental and clinical results [46–49].

3. Methods

We performed four independent MD simulations of wild-type and mutated GTP-bound KRas-4B-Far attached to DOPC/DOPS (4:1) bilayers. Eventually, some of the lipids were replaced by cholesterol molecules in such a way that two cholesterol percentages were considered: 0% and 30%. Each system contains a total of 304 lipid molecules fully solvated by 60,000 TIP3P water molecules and 48 potassium chloride at the human body concentration (0.15 M), yielding a system size of 222,000 atoms. All MD inputs were generated using CHARMM-GUI web-based tool [68]. The force field was CHARMM36m for proteins [69] and CHARMM36 [70] for other molecules in each system. The crystal structure of KRas-4B with the partially disordered hypervariable region (pdb 5TB5) and GTP (pdb 5VQ2) were used to generate full-length GTP-bound KRas-4B-Far proteins. Two sequences of the wild-type and oncogenic KRas-4B-Far are presented in Fig. A6.

After model building, each system was energy minimized for 5000 steps followed by three 250 ps simulations, and then four additional 500 ps equilibrium runs while gradually reducing the harmonic constraints on the systems. We used the NPT ensemble with the constant pressure of 1 atm maintained by the Parrinello-Rahman piston method with a damping coefficient of 5 ps^{-1} and temperature of 310.15 K controlled by the Nosé-Hoover thermostat method with a damping coefficient of 1 ps^{-1}. Meaningful production runs were performed with an NPT ensemble for 1 μs from the last configuration of equilibrium run for each system, for a total of 4 μs. Time steps of 2 fs were used in all production simulations and the particle mesh Ewald method with a Coulomb radius of 1.2 nm was employed to compute long-ranged electrostatic interactions. The cutoff for Lennard-Jones interactions was set to 1.2 nm. In all MD simulations, the GROMACS/2018.3 package was employed [71] and periodic boundary conditions in three directions of space have been taken.

4. Conclusions

In this work, we performed MD simulations on four systems of wild-type/oncogenic KRas-4B-Far protein binding to membranes with different cholesterol contents (0% and 30%) to study the influence of cholesterol on the orientation of KRas. KRas-4B-Far shows the condensing effect on the area per lipid of the anionic model membrane through strong interactions between its CD and HVR moieties with the head groups of the lipids. More flexibility in its CD structure of KRas-4B-Far has been observed when binding to the PM with high cholesterol concentration, for both wild-type and mutant KRas-4B-Far proteins. The reorientation of mutant KRas-4B-Far on the anionic cholesterol-30% model membrane has been observed during the 500 ns simulations time, giving a hint on the low free energy barriers between a pair of orientation states (e.g. OS_1-OS_0, and OS_0-OS_2).

It has been shown for the first time that cholesterol makes it much easier for the mutant G12D-PHOS-KRas-4B-Far shifting between different orientation states. The high cholesterol content in the PM favors OS_1, exposing the effector-binding loop for signal transduction in cells from the atomic level. We propose that during the treatment of KRas-4B-related cancers, reducing the cholesterol level in the PM and sustaining cancer progression by controlling the plasma cholesterol intake should be taken into account in anti-cancer therapies. The present study of the role of cholesterol in Kras-4B orientation can provide one more direction and method for the treatment and prevention of cancer. By conducting 4 μs MD simulations, we confirm that high cholesterol in the PM helps KRas-4B mutant stays in its constitutively active state, which suggests that high cholesterol intake can increase the mortality and may promote cancer progression for cancer patients.

Author Contributions: Data curation, Huixia Lu, Jordi Martí; formal analysis, Huixia Lu, Jordi Martí; funding acquisition, Jordi Martí; investigation, Huixia Lu, Jordi Martí; project administration, Jordi Martí; software, Huixia Lu, Jordi Martí; supervision, Jordi Martí; writing–original draft preparation, Huixia Lu, Jordi Martí; writing–review and editing, Huixia Lu, Jordi Martí.

Preprints (www.preprints.org) | NOT PEER-REVIEWED | Posted: 12 October 2020 doi:10.20944/preprints202010.0239.v1

Acknowledgments: We thank financial support provided by the Spanish Ministry of Science, Innovation, and Universities (project number PGC2018-099277-B-C21, funds MCIU/AEI/FEDER, UE). Huixia Lu is a Ph.D. fellow from the Chinese Scholarship Council (grant 201607040059). We also acknowledge the use of computer resources from the "Barcelona Supercomputing Center-Red Espanola de Supercomputacion" through projects FI-2019-3-0008 and FI-2019-2-0004.

Conflicts of Interest: The authors declare no conflict of interest.

Abbreviations

The following abbreviations are used in this manuscript:

DOPC	1,2-dioleoyl-sn-glycero-3-phosphocholine
DOPS	1,2-dioleoyl-sn-glycero-3-phospho-L-serine
GDP	guanosine diphosphate
GTP	guanosine triphosphate
PM	plasma membrane
GEF	Guanine-nucleotide-exchange factors
GAP	GTPase-activating proteins
COSMIC	Catalog of Somatic Mutations in Cancer
HVR	hypervariable region
FAR	farnesyl group
CD	catalytic domain
PHOS	phosphorylated serine
PTMs	post-translational modifications
OS	orientation states

Appendix A. Supporting information

Appendix A.1. Area per lipid

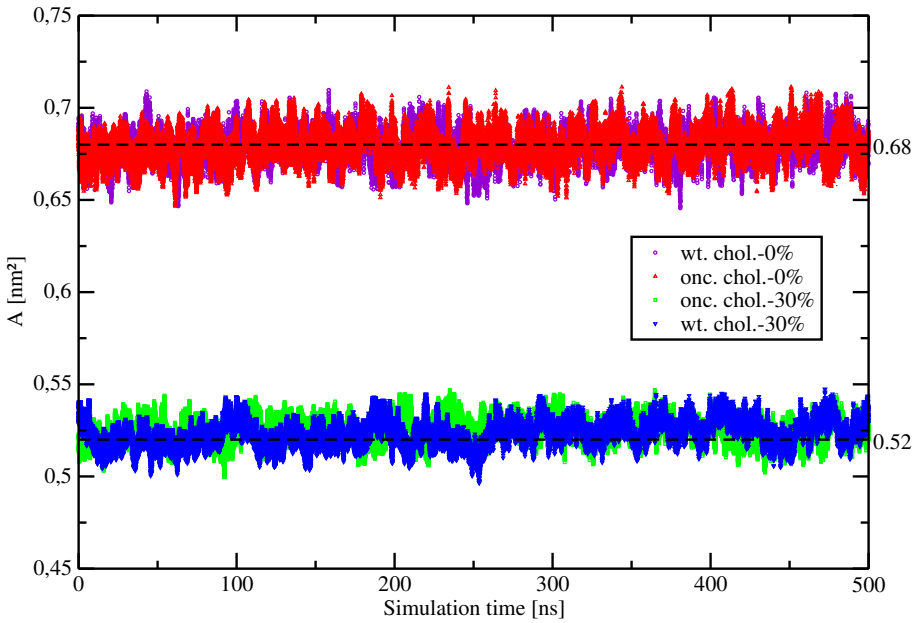

Figure A1. Area per lipid of four wild-type/mutant KRas-4B-Far systems with different content of cholesterol as a function of simulation time. The black dashed line indicates the average value for each system of the second half of the total 1000 ns production runs.

Preprints (www.preprints.org) | NOT PEER-REVIEWED | Posted: 12 October 2020 doi:10.20944/preprints202010.0239.v1

Appendix A.2. Orientation of KRas on the PM

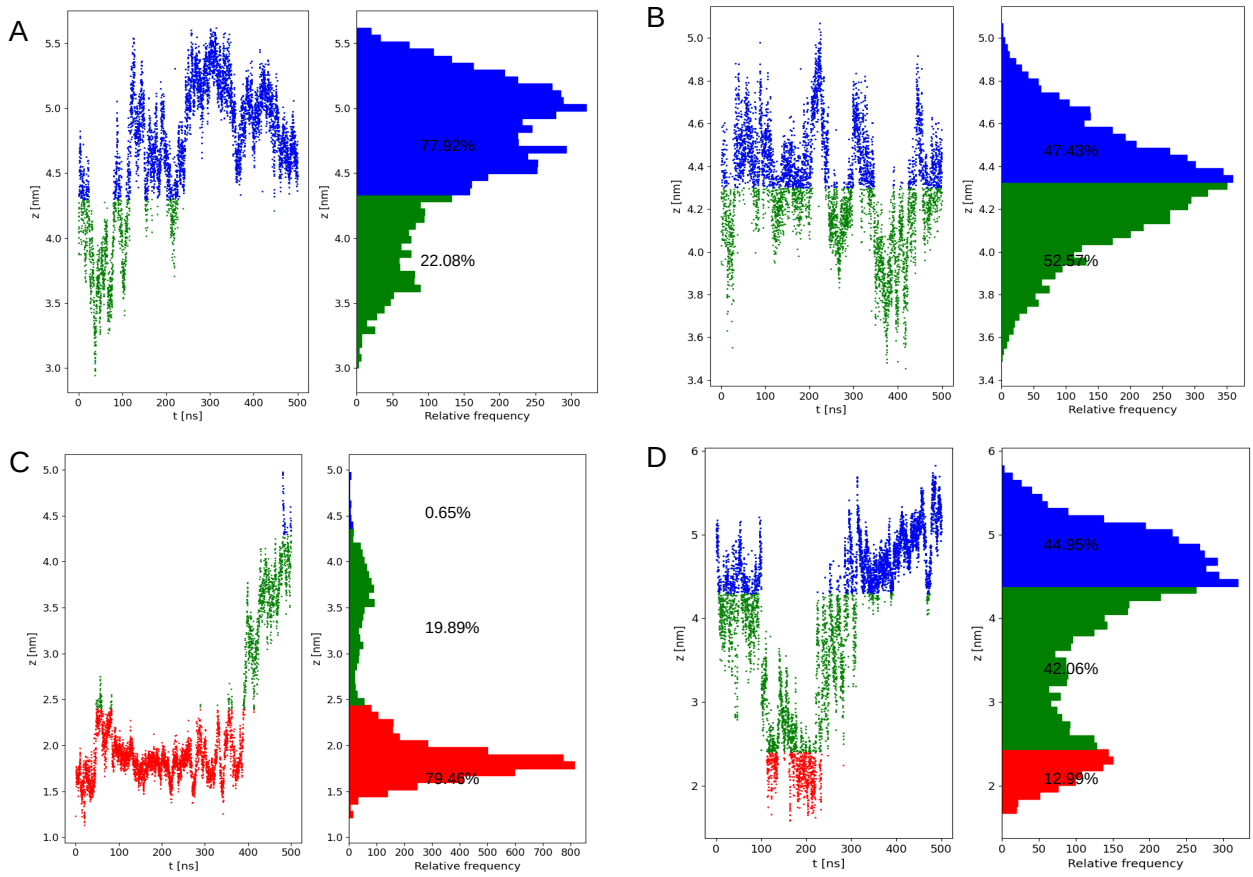

Figure A2. Time evolution of z during the last 500 ns MD simulation of GTP-bound G12D-PHOS-KRas-Far. The ratios of the different regions defined in Ref. [17] of the distance are shown on each panel. Three different pools of conformational states are depicted in different colors: z ∈ [0, 2.4) in red, z ∈ [2.4, 4.3] in green, and z ∈ (4.3,] in blue. A panel refers to onc. chol.-0%, B refers to the wt. chol.-0% system, C panel stands for the onc. chol.-30% system, and D represents the wt. chol.-30% system, respectively.

Preprints (www.preprints.org) | NOT PEER-REVIEWED | Posted: 12 October 2020 doi:10.20944/preprints202010.0239.v1

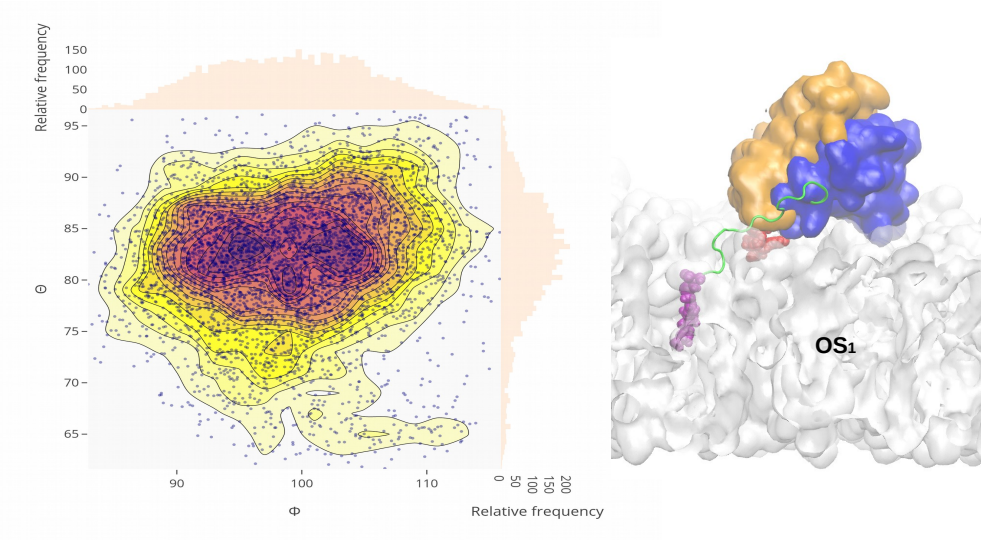

Figure A3. Orientation of the mutant KRas-4B-Far on the cholesterol-free membrane. Colors defined as Fig. 5.

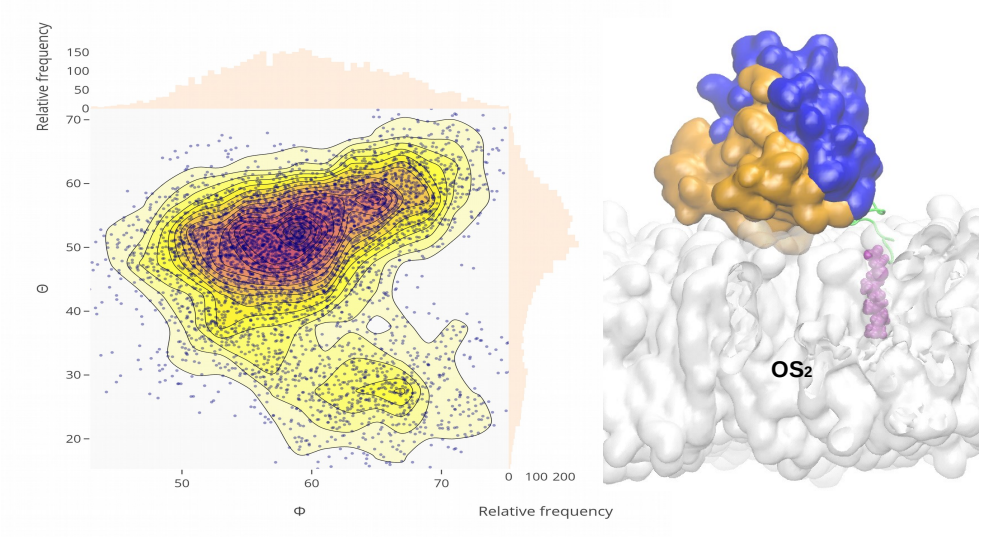

Figure A4. Orientation of the wild-type KRas-4B-Far on the cholesterol-free membrane. Colors defined as Fig. 5.

Preprints (www.preprints.org) | NOT PEER-REVIEWED | Posted: 12 October 2020 doi:10.20944/preprints202010.0239.v1

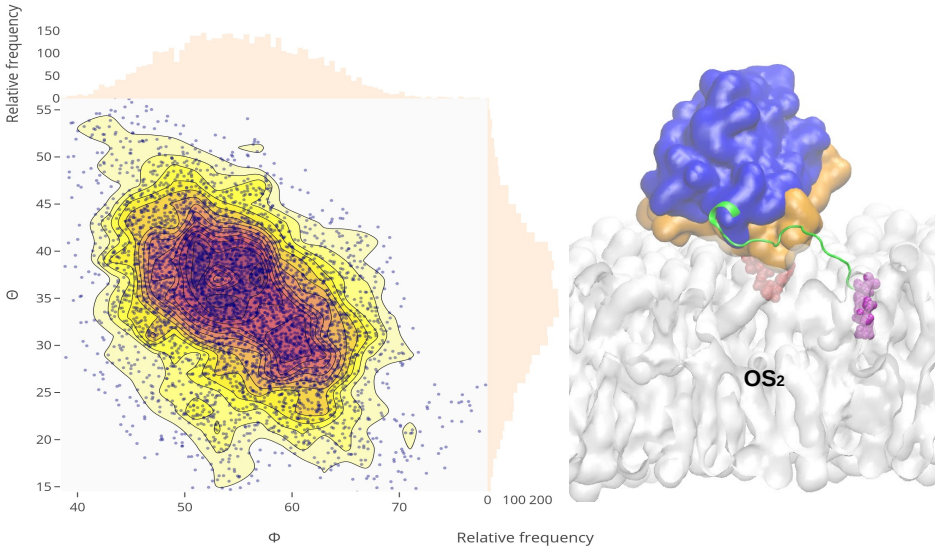

Figure A5. Orientation of the wild-type KRas-4B-Far on the anionic cholesterol-30% membrane. Colors defined as Fig. 5.

Appendix A.3. Sequences of wild-type and mutant KRas-4B-Far proteins

Here in Fig. A6, sequences for wild-type and mutated KRas-4B-Far are presented.

Sequence of wild-type KRas-4B-Far:

10 20 30 40 50 60 70 80 90

MTEYKLVVVGAGGVGKSALTIQLIQNHFVDEYDPTIEDSYRKQVVIDGETCLLDILDTAGQEEYSAMRDQYMRTGEGFLCVFAINNTKSFEDIHH

YREQIKRVKDSEDVPMVLVGNKCDLPSRTVDTKQAQDLARSYGIPFIETSAKTRQGVDDAFYTLVREIRKHKEKMSKDGKKKKKKSKTKC$_f$

100 110 120 130 140 150 160 170 180

Sequence of oncogenic KRas-4B-Far:

10 20 30 40 50 60 70 80 90

MTEYKLVVVGADGVGKSALTIQLIQNHFVDEYDPTIEDSYRKQVVIDGETCLLDILDTAGQEEYSAMRDQYMRTGEGFLCVFAINNTKSFEDIHH

YREQIKRVKDSEDVPMVLVGNKCDLPSRTVDTKQAQDLARSYGIPFIETSAKTRQGVDDAFYTLVREIRKHKEKMSKDGKKKKKKSpKTKC$_f$

100 110 120 130 140 150 160 170 180

Figure A6. Two sequences of oncogenic and wild-type KRas-4B-Far. Mutated sites are in red color. Here C_f denotes the farnesylated Cys-185 and S_p represents the phosphorylated Ser-181 site.

References

1. McLaughlin, S.; Murray, D. Plasma membrane phosphoinositide organization by protein electrostatics. *Nature* **2005**, *438*, 605–611.
2. Ingólfsson, H.I.; Melo, M.N.; Van Eerden, F.J.; Arnarez, C.; Lopez, C.A.; Wassenaar, T.A.; Periole, X.; De Vries, A.H.; Tieleman, D.P.; Marrink, S.J. Lipid organization of the plasma membrane. *Journal of the american chemical society* **2014**, *136*, 14554–14559.
3. Zhang, Y.; Chen, X.; Gueydan, C.; Han, J. Plasma membrane changes during programmed cell deaths. *Cell research* **2018**, *28*, 9–21.
4. Krapf, D. Compartmentalization of the plasma membrane. *Current opinion in cell biology* **2018**, *53*, 15–21.
5. Zhang, J.; Jin, R.; Jiang, D.; Chen, H.Y. Electrochemiluminescence-based capacitance microscopy for label-free imaging of antigens on the cellular plasma membrane. *Journal of the American Chemical Society* **2019**, *141*, 10294–10299.
6. Nussinov, R.; Tsai, C.J.; Jang, H. Oncogenic Ras isoforms signaling specificity at the membrane. *Cancer research* **2018**, *78*, 593–602.
7. Bernards, A.; Settleman, J. GAP control: regulating the regulators of small GTPases. *Trends in cell biology* **2004**, *14*, 377–385.
8. Wennerberg, K.; Rossman, K.L.; Der, C.J. The Ras superfamily at a glance. *Journal of cell science* **2005**, *118*, 843–846.
9. Schmidt, A.; Hall, A. Guanine nucleotide exchange factors for Rho GTPases: turning on the switch. *Genes & development* **2002**, *16*, 1587–1609.
10. Stephen, A.G.; Esposito, D.; Bagni, R.K.; McCormick, F. Dragging ras back in the ring. *Cancer cell* **2014**, *25*, 272–281.
11. Forbes, S.A.; Bindal, N.; Bamford, S.; Cole, C.; Kok, C.Y.; Beare, D.; Jia, M.; Shepherd, R.; Leung, K.; Menzies, A.; others. COSMIC: mining complete cancer genomes in the Catalogue of Somatic Mutations in Cancer. *Nucleic acids research* **2010**, *39*, D945–D950.
12. Hobbs, G.A.; Der, C.J.; Rossman, K.L. RAS isoforms and mutations in cancer at a glance. *Journal of cell science* **2016**, *129*, 1287–1292.
13. Gelabert-Baldrich, M.; Soriano-Castell, D.; Calvo, M.; Lu, A.; Viña-Vilaseca, A.; Rentero, C.; Pol, A.; Grinstein, S.; Enrich, C.; Tebar, F. Dynamics of KRas on endosomes: involvement of acidic phospholipids in its association. *The FASEB Journal* **2014**, *28*, 3023–3037.
14. Cho, K.j.; van der Hoeven, D.; Zhou, Y.; Maekawa, M.; Ma, X.; Chen, W.; Fairn, G.D.; Hancock, J.F. Inhibition of acid sphingomyelinase depletes cellular phosphatidylserine and mislocalizes K-Ras from the plasma membrane. *Molecular and cellular biology* **2016**, *36*, 363–374.
15. Gregory, M.C.; McLean, M.A.; Sligar, S.G. Interaction of KRas4b with anionic membranes: A special role for PIP2. *Biochemical and biophysical research communications* **2017**, *487*, 351–355.
16. Zhou, Y.; Wong, C.O.; Cho, K.j.; Van Der Hoeven, D.; Liang, H.; Thakur, D.P.; Luo, J.; Babic, M.; Zinsmaier, K.E.; Zhu, M.X.; others. Membrane potential modulates plasma membrane phospholipid dynamics and K-Ras signaling. *Science* **2015**, *349*, 873–876.
17. Prakash, P.; Litwin, D.; Liang, H.; Sarkar-Banerjee, S.; Dolino, D.; Zhou, Y.; Hancock, J.F.; Jayaraman, V.; Gorfe, A.A. Dynamics of membrane-bound G12V-KRAS from simulations and single-molecule FRET in native nanodiscs. *Biophysical journal* **2019**, *116*, 179–183.
18. Prakash, P.; Zhou, Y.; Liang, H.; Hancock, J.F.; Gorfe, A.A. Oncogenic K-Ras binds to an anionic membrane in two distinct orientations: a molecular dynamics analysis. *Biophysical journal* **2016**, *110*, 1125–1138.
19. Prakash, P.; Gorfe, A.A. Probing the conformational and energy landscapes of KRAS membrane orientation. *The Journal of Physical Chemistry B* **2019**, *123*, 8644–8652.
20. Tsai, C.J.; Ma, B.; Sham, Y.Y.; Kumar, S.; Nussinov, R. Structured disorder and conformational selection. *Proteins: Structure, Function, and Bioinformatics* **2001**, *44*, 418–427.
21. Lu, H.; Marti, J. Long-lasting salt bridges provide the anchoring mechanism of oncogenic KRas-4B at cell membranes. *bioRxiv* **2020**, [https://www.biorxiv.org/content/early/2020/08/14/2020.08.14.250738.full.pdf]. doi:10.1101/2020.08.14.250738.

22. Cao, S.; Chung, S.; Kim, S.; Li, Z.; Manor, D.; Buck, M. K-Ras G-domain binding with signaling lipid phosphatidylinositol (4, 5)-phosphate (PIP2): membrane association, protein orientation, and function. *Journal of Biological Chemistry* **2019**, *294*, 7068–7084.
23. Yang, M.H.; Laurent, G.; Bause, A.S.; Spang, R.; German, N.; Haigis, M.C.; Haigis, K.M. HDAC6 and SIRT2 regulate the acetylation state and oncogenic activity of mutant K-RAS. *Molecular Cancer Research* **2013**, *11*, 1072–1077.
24. Lu, S.; Jang, H.; Gu, S.; Zhang, J.; Nussinov, R. Drugging Ras GTPase: a comprehensive mechanistic and signaling structural view. *Chemical Society Reviews* **2016**, *45*, 4929–4952.
25. Ahearn, I.M.; Haigis, K.; Bar-Sagi, D.; Philips, M.R. Regulating the regulator: post-translational modification of RAS. *Nature reviews Molecular cell biology* **2012**, *13*, 39–51.
26. Zhou, B.; Cox, A.D. Posttranslational Modifications of Small G Proteins. In *Ras Superfamily Small G Proteins: Biology and Mechanisms 1*; Springer, 2014; pp. 99–131.
27. Abdelkarim, H.; Banerjee, A.; Grudzien, P.; Leschinsky, N.; Abushaer, M.; Gaponenko, V. The Hypervariable Region of K-Ras4B Governs Molecular Recognition and Function. *International journal of molecular sciences* **2019**, *20*, 5718.
28. Ahearn, I.; Zhou, M.; Philips, M.R. Posttranslational modifications of RAS proteins. *Cold Spring Harbor perspectives in medicine* **2018**, p. a031484.
29. Konstantinopoulos, P.A.; Karamouzis, M.V.; Papavassiliou, A.G. Post-translational modifications and regulation of the RAS superfamily of GTPases as anticancer targets. *Nature reviews Drug discovery* **2007**, *6*, 541–555.
30. Zhang, S.Y.; Sperlich, B.; Li, F.Y.; Al-Ayoubi, S.; Chen, H.X.; Zhao, Y.F.; Li, Y.M.; Weise, K.; Winter, R.; Chen, Y.X. Phosphorylation weakens but does not inhibit membrane binding and clustering of K-Ras4B. *ACS chemical biology* **2017**, *12*, 1703–1710.
31. Alvarez-Moya, B.; Lopez-Alcala, C.; Drosten, M.; Bachs, O.; Agell, N. K-Ras4B phosphorylation at Ser181 is inhibited by calmodulin and modulates K-Ras activity and function. *Oncogene* **2010**, *29*, 5911–5922.
32. Bivona, T.G.; Quatela, S.E.; Bodemann, B.O.; Ahearn, I.M.; Soskis, M.J.; Mor, A.; Miura, J.; Wiener, H.H.; Wright, L.; Saba, S.G.; others. PKC regulates a farnesyl-electrostatic switch on K-Ras that promotes its association with Bcl-XL on mitochondria and induces apoptosis. *Molecular cell* **2006**, *21*, 481–493.
33. Kollár, P.; Rajchard, J.; Balounová, Z.; Pazourek, J. Marine natural products: bryostatins in preclinical and clinical studies. *Pharmaceutical biology* **2014**, *52*, 237–242.
34. Barceló, C.; Paco, N.; Morell, M.; Alvarez-Moya, B.; Bota-Rabassedas, N.; Jaumot, M.; Vilardell, F.; Capella, G.; Agell, N. Phosphorylation at Ser-181 of oncogenic KRAS is required for tumor growth. *Cancer research* **2014**, *74*, 1190–1199.
35. Jang, H.; Abraham, S.J.; Chavan, T.S.; Hitchinson, B.; Khavrutskii, L.; Tarasova, N.I.; Nussinov, R.; Gaponenko, V. Mechanisms of membrane binding of small GTPase K-Ras4B farnesylated hypervariable region. *Journal of Biological Chemistry* **2015**, *290*, 9465–9477.
36. Alvarez-Moya, B.; Barceló, C.; Tebar, F.; Jaumot, M.; Agell, N. CaM interaction and Ser181 phosphorylation as new K-Ras signaling modulators. *Small GTPases* **2011**, *2*, 5911–5922.
37. Dharmaiah, S.; Bindu, L.; Tran, T.H.; Gillette, W.K.; Frank, P.H.; Ghirlando, R.; Nissley, D.V.; Esposito, D.; McCormick, F.; Stephen, A.G.; others. Structural basis of recognition of farnesylated and methylated KRAS4b by PDEδ. *Proceedings of the National Academy of Sciences* **2016**, *113*, E6766–E6775.
38. Schmick, M.; Vartak, N.; Papke, B.; Kovacevic, M.; Truxius, D.C.; Rossmannek, L.; Bastiaens, P.I. KRas localizes to the plasma membrane by spatial cycles of solubilization, trapping and vesicular transport. *Cell* **2014**, *157*, 459–471.
39. Zimmermann, G.; Papke, B.; Ismail, S.; Vartak, N.; Chandra, A.; Hoffmann, M.; Hahn, S.A.; Triola, G.; Wittinghofer, A.; Bastiaens, P.I.; others. Small molecule inhibition of the KRAS–PDEδ interaction impairs oncogenic KRAS signalling. *Nature* **2013**, *497*, 638–642.
40. Muratcioglu, S.; Jang, H.; Gursoy, A.; Keskin, O.; Nussinov, R. PDEδ binding to Ras isoforms provides a route to proper membrane localization. *The Journal of Physical Chemistry B* **2017**, *121*, 5917–5927.
41. Murarka, S.; Martín-Gago, P.; Schultz-Fademrecht, C.; Al Saabi, A.; Baumann, M.; Fansa, E.K.; Ismail, S.; Nussbaumer, P.; Wittinghofer, A.; Waldmann, H. Development of pyridazinone chemotypes targeting the PDEδ prenyl binding site. *Chemistry–A European Journal* **2017**, *23*, 6083–6093.

42. Ntai, I.; Fornelli, L.; DeHart, C.J.; Hutton, J.E.; Doubleday, P.F.; LeDuc, R.D.; van Nispen, A.J.; Fellers, R.T.; Whiteley, G.; Boja, E.S.; others. Precise characterization of KRAS4b proteoforms in human colorectal cells and tumors reveals mutation/modification cross-talk. *Proceedings of the National Academy of Sciences* **2018**, *115*, 4140–4145.
43. McMullen, T.P.; Lewis, R.N.; McElhaney, R.N. Cholesterol–phospholipid interactions, the liquid-ordered phase and lipid rafts in model and biological membranes. *Current opinion in colloid & interface science* **2004**, *8*, 459–468.
44. Levitan, I.; Fang, Y.; Rosenhouse-Dantsker, A.; Romanenko, V. Cholesterol and ion channels. In *Cholesterol Binding and Cholesterol Transport Proteins:*; Springer, 2010; pp. 509–549.
45. Ding, X.; Zhang, W.; Li, S.; Yang, H. The role of cholesterol metabolism in cancer. *American journal of cancer research* **2019**, *9*, 219.
46. Boughter, C.T.; Monje-Galvan, V.; Im, W.; Klauda, J.B. Influence of cholesterol on phospholipid bilayer structure and dynamics. *The Journal of Physical Chemistry B* **2016**, *120*, 11761–11772.
47. Kim, S.W.; Wiers, C.E.; Tyler, R.; Shokri-Kojori, E.; Jang, Y.J.; Zehra, A.; Freeman, C.; Ramirez, V.; Lindgren, E.; Miller, G.; others. Influence of alcoholism and cholesterol on TSPO binding in brain: PET [11 C] PBR28 studies in humans and rodents. *Neuropsychopharmacology* **2018**, *43*, 1832–1839.
48. Chen, H.; Qin, S.; Wang, M.; Zhang, T.; Zhang, S. Association between cholesterol intake and pancreatic cancer risk: evidence from a meta-analysis. *Scientific reports* **2015**, *5*, 8243.
49. Huang, B.Z.; Chang, J.I.; Li, E.; Xiang, A.H.; Wu, B.U. Influence of statins and cholesterol on mortality among patients with pancreatic cancer. *JNCI: Journal of the National Cancer Institute* **2017**, *109*.
50. Poger, D.; Mark, A.E. On the validation of molecular dynamics simulations of saturated and cis-monounsaturated phosphatidylcholine lipid bilayers: a comparison with experiment. *Journal of Chemical Theory and Computation* **2010**, *6*, 325–336.
51. Lütgebaucks, C.; Macias-Romero, C.; Roke, S. Characterization of the interface of binary mixed DOPC: DOPS liposomes in water: The impact of charge condensation. *The Journal of chemical physics* **2017**, *146*, 044701.
52. Novakova, E.; Giewekemeyer, K.; Salditt, T. Structure of two-component lipid membranes on solid support: An x-ray reflectivity study. *Physical Review E* **2006**, *74*, 051911.
53. Chaban, V. Computationally efficient prediction of area per lipid. *Chemical Physics Letters* **2014**, *616*, 25–29.
54. Petrache, H.I.; Tristram-Nagle, S.; Gawrisch, K.; Harries, D.; Parsegian, V.A.; Nagle, J.F. Structure and fluctuations of charged phosphatidylserine bilayers in the absence of salt. *Biophysical journal* **2004**, *86*, 1574–1586.
55. Lu, H.; Martí, J. Binding and dynamics of melatonin at the interface of phosphatidylcholine-cholesterol membranes. *PloS one* **2019**, *14*, e0224624.
56. Litz, J.P.; Thakkar, N.; Portet, T.; Keller, S.L. Depletion with cyclodextrin reveals two populations of cholesterol in model lipid membranes. *Biophysical journal* **2016**, *110*, 635–645.
57. Kufareva, I.; Abagyan, R. Methods of protein structure comparison. In *Homology Modeling*; Springer, 2011; pp. 231–257.
58. Abankwa, D.; Gorfe, A.A.; Inder, K.; Hancock, J.F. Ras membrane orientation and nanodomain localization generate isoform diversity. *Proceedings of the National Academy of Sciences* **2010**, *107*, 1130–1135.
59. Kapoor, S.; Triola, G.; Vetter, I.R.; Erlkamp, M.; Waldmann, H.; Winter, R. Revealing conformational substates of lipidated N-Ras protein by pressure modulation. *Proceedings of the National Academy of Sciences* **2012**, *109*, 460–465.
60. Mazhab-Jafari, M.T.; Marshall, C.B.; Smith, M.J.; Gasmi-Seabrook, G.M.; Stathopulos, P.B.; Inagaki, F.; Kay, L.E.; Neel, B.G.; Ikura, M. Oncogenic and RASopathy-associated K-RAS mutations relieve membrane-dependent occlusion of the effector-binding site. *Proceedings of the National Academy of Sciences* **2015**, *112*, 6625–6630.
61. Yan, S.; Qu, X.; Xu, L.; Che, X.; Ma, Y.; Zhang, L.; Teng, Y.; Zou, H.; Liu, Y. Bufalin enhances TRAIL-induced apoptosis by redistributing death receptors in lipid rafts in breast cancer cells. *Anti-cancer drugs* **2014**, *25*, 683–689.
62. Kuzu, O.F.; Noory, M.A.; Robertson, G.P. The role of cholesterol in cancer. *Cancer research* **2016**, *76*, 2063–2070.

 doi:10.20944/preprints202010.0239.v1

63. Ravnskov, U.; Rosch, P.J.; McCully, K.S. Statins do not protect against cancer: quite the opposite. *J Clin Oncol* **2015**, *33*, 810–1.
64. Ravnskov, U.; McCully, K.; Rosch, P. The statin-low cholesterol-cancer conundrum. *QJM: An International Journal of Medicine* **2012**, *105*, 383–388.
65. Nielsen, S.F.; Nordestgaard, B.G.; Bojesen, S.E. Statin use and reduced cancer-related mortality. *New England Journal of Medicine* **2012**, *367*, 1792–1802.
66. Radišauskas, R.; Kuzmickienė, I.; Milinavičienė, E.; Everatt, R. Hypertension, serum lipids and cancer risk: A review of epidemiological evidence. *Medicina* **2016**, *52*, 89–98.
67. Murai, T. Cholesterol lowering: role in cancer prevention and treatment. *Biological chemistry* **2015**, *396*, 1–11.
68. Jo, S.; Kim, T.; Iyer, V.G.; Im, W. CHARMM-GUI: a web-based graphical user interface for CHARMM. *Journal of computational chemistry* **2008**, *29*, 1859–1865.
69. Huang, J.; Rauscher, S.; Nawrocki, G.; Ran, T.; Feig, M.; de Groot, B.L.; Grubmüller, H.; MacKerell, A.D. CHARMM36m: an improved force field for folded and intrinsically disordered proteins. *Nature methods* **2017**, *14*, 71–73.
70. Huang, J.; MacKerell Jr, A.D. CHARMM36 all-atom additive protein force field: Validation based on comparison to NMR data. *Journal of computational chemistry* **2013**, *34*, 2135–2145.
71. Lemkul, J. From proteins to perturbed Hamiltonians: A suite of tutorials for the GROMACS-2018 molecular simulation package [article v1. 0]. *Living Journal of Computational Molecular Science* **2018**, *1*, 5068.